An analytical approach in estimating different base fluids for silicon dioxide nanofluid to effectively cool Li-ion battery pack

[1]Prajwal Thorat*,[2]Prof.Dr.Sudarshan Sanap,[2]Prof.Shashank Gawade,[3]Prof.Dr.Rahul Kadu
[1]PG Student,[2]Mechanical Engg.Dept.,School of Engineering & Sciences,Pune,Maharashtra,India,[3]Applied Sciences & Humanities Dept.,School of Engineering & Sciences,Pune,Maharashtra,India
[1]prajwalthorat596@gmail.com

***Abstract*—Thermal management systems of Lithium-ion battery packs are focused upon in recent times due to fire-related issues generated at higher temperatures particularly above the operating temperature limits of Lithium-ion batteries. The combination of high temperature, flammable gases, and heat-producing reactions exacerbate thermal runaway. In order to tackle this issue, many automotive manufactures are using an indirect liquid cooling technique to maintain the battery pack within the operating temperature limits. Coolants such as water, ethylene glycol and mixture of water and ethylene glycol are used, but the performance in cooling the battery pack is not satisfactory. Thus, in order to tackle these issues silicon dioxide nanofluid is focused upon as coolant which is expected to cool the battery pack more efficiently. Nanofluids are engineered fluids that contain suspended nanoparticles, which are expected to enhance their thermo physical properties. The current research work focus on finding the best suited base fluid for suspending the nanofluid and results have shown that 70:30 water-ethylene glycol mixture can be the most optimized choice having temperature reduction of 39.94 º C with freezing and boiling temperatures of -13.7 º C and 104 º C respectively suited for battery cooling applications.**

Keywords—Thermal Runaway, Thermo physical properties, Liquid Cooling, Nanofluids

I. INTRODUCTION

The challenges with fossil fuel technology vehicles are growing day by day. Today most of the automobiles running on roads are Internal Combustion Engines (I.C.E) vehicles. The I.C.E vehicles are still the most promising technology due to advantages and ease it offers but however during recent decades the challenges with fossil fuel technology is increasing at a rapid rate.[1] The emissions produced due to daily commute is rising at an alarming rate and can certainly harm the environment on a whole. Another challenge that these I.C.E face is its availability and decreasing reserves over the globe. The reserves of fossil fuels might reach its extinction in near future and thus efforts must be taken to overcome it. The third challenge regarding the use of fossil fuels is that due to its higher demand and lesser supply the cost of these fuels is on a higher side and is expected to increase in near future. [2] Thus in order to address this challenges, researchers and automotive makers have come up with an alternative and greener technology by introducing Electric Vehicles (EVs) into the market. The insurgence of EVs is not new but dated before the invention of I.C.E vehicles to the world. [3] The reasons for growing popularity of I.C.E vehicles as compared to EVs during and after its invention is the lesser range offered by the vehicle in single charge along with lower value of energy density. The energy density refers to the ability of the battery to store energy per unit volume. The development of power electronics sector during that time was not up to the mark as compared to the technology developed today.[4] However later due to the development in the field of battery technology and power electronics sector paved way for the growth of EV industry to much larger extend. The evolution of battery technology started right from the Lead-acid battery to the most used batteries nowadays the Li-ion batteries. The subsections below will describe the Lithium-ion and Lithium Iron Phosphate (LiFePO4) battery technology in EV technology in detail.[5] The authors have discussed the challenges and opportunities in the electric vehicle industry. The authors have depicted the percentage sale of different EVs in European Union and surrounding regions. The authors have elaborated the schemes and policies to increase the adoption and use of EVs. The authors have concluded that the development of EV sector across the globe is subject to addressing the issues and challenges to finding solution in common. [6] The authors have discussed the use of Li-ion batteries in hybrid as well as battery electric vehicles. The challenges of Li-ion battery technologies such as cost, charging time, safety and recycling are focused upon. The authors have also discussed the impact on batteries at cold climatic conditions and have inferred that internal impedance increases and capacity of cell starts to degrade. The current

 e-ISSN No. 2584-1025

study aims to address the issues related to thermal runaway in $LiFePO_4$ battery pack. This paper discusses the different battery technologies used in EVs along with their thermal issues. The heat generation and maximum temperature reached by the battery pack is calculated using analytical equations and Modified Indian Drive Cycle (MIDC) data respectively. The current study also focuses on the use of Nanofluids as coolant due to enhanced thermo physical properties mainly as the higher thermal conductivity value leads to higher heat dissipation rate causing higher heat removal from the battery pack and maintain the battery pack within operating temperature ranges for optimal performance. The current study tries to focus on the use of Fly ash as material for cooling the battery pack. Finally, results are tabulated based on analytical calculations and the best nanofluid is chosen for battery cooling applications.

II. LITHIUM-IRON PHOSPHATE BATTERIES

The invention of Lithium-iron phosphate ($LiFePO_4$) battery leads to widen the spectrum of Li-ion battery technology in electric vehicles as well as other energy storage applications.[7] The electrochemical reaction inside the ($LiFePO_4$) battery can be explained and represented as follows,:

Discharge Operation:

$$LiFePo_4 \text{ ----------} > Li^+ + FePO_4^-$$

Charging Operation:

$$Li^+ + FePO_4 \text{ }^{-\text{----------}} > LiFePO4$$

The operation causing release of energy during discharge is mainly concerned with movement of Li-ion from the anode to the cathode basically ($LiFePO_4$) through the electrolyte. The electrons travel through the external circuit thereby supplying the stored energy. [8] During charging operations the reactions are reversed. The Fig.1. Represents Charge-Discharge operation for $LiFePO_4$ battery. There are certain advantages that $LiFePO_4$ batteries pave way for and they are as follows, the excellent stability against thermal effects makes $LiFePO_4$ batteries best choice for usage and hereby reduces the risk of uncontrolled combustion. The one of the best advantage that $LiFePO_4$ batteries provide is longer cycle life than traditionally used Li-ion batteries. The longer the charge-discharge cycle of $LiFePO_4$ highlights its use in electric vehicles as well as in other energy storage applications. The capability of $LiFePO_4$ batteries to provide stable voltage output marks its importance in continuous charge-discharge cycles. Though LFP batteries possess many advantages there are certain challenges that must be focused upon, they are as follows, the LFP batteries may tend to possess lower energy density as compared to many other cell chemistries and thus research is going on to improve the value of energy density. The LFP batteries tend to possess a voltage plateau referring to a region with constant voltage operating region. However, some applications may require a broad range of operating voltages and researchers are focusing to address this issue. The cost of $LiFePO_4$ batteries are on a higher side as compared to other Li-ion cell chemistries and thus scale in $LiFePO_4$ battery manufacturing can certainly lead to reduction in cost.

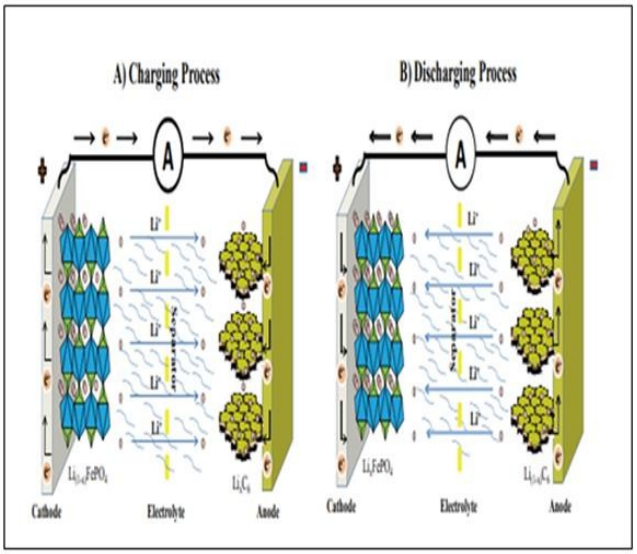

Fig.1. Represents Charge-Discharge operations for LiFePO4 battery [7]

The use of $LiFePO_4$ batteries is growing at an alarming rate in residential, industrial as well as commercial use. The growth of $LiFePO_4$ battery market is mainly dependent on policies developed for its promotion, modernizing grid for energy transmission and reliable backup power supply. Overheating and thermal issues in EVs is predominant and thus use of appropriate batteries is important.

III. THERMAL RUNAWAY & BATTERY COOLING TECHNIQUES

Though the use of Li-ion and $LiFePO_4$ batteries is increasing rapidly, there are certain challenges that must be addressed and worked upon. [9] The three major challenges faced by these batteries are as follows, requiring larger time to charge and discharge the batteries, these cells or batteries works well within certain operating range of temperatures above or below which can hamper the performance of cell or battery and may lead to its degradation. As discussed earlier, these Li-ion and $LiFePO_4$ cells work well within certain range of operating temperatures.[10] The range of operating temperatures for Li-ion is from – 20 ^{o} C to 65 ^{o} C and $LiFePO_4$ is from – 20 ^{o} C to 45 ^{o} C respectively. The value of temperatures above or below these ranges can affect the cell and may lead to thermal runaway causing smoke and bursting of cells. Thermal runaway is mainly caused due to three main types of abuses namely Mechanical abuse, Electrical abuse and Thermal abuse. The Fig.2. Represents different causes for Thermal runaway in Li-ion batteries. Mechanical abuse is mainly caused due to penetration and crushing of Li-ion or $LiFePO_4$ batteries. The event of crush and penetration can happen during accident of vehicle or dropping of battery pack from height can lead to mechanical abuse. The electrical abuse is mainly due to short-circuiting of cells in battery pack or due to overcharging of cells for longer duration of time. The

electrical abuse is mainly caused due to improper electrical connections or due to lack of insulation provided between live parts.[11] Thermal abuse is mainly due to ageing of cells and operating the cells above its safe operating zone. The rise in temperature of cells is mainly due to high current demand from the battery pack. Among the above three abuses the thermal abuse is the most fatal of all causing unforeseen impact on the battery pack. The rising temperature of cell may leads to breakdown of electrolyte and thermal decomposition of cathodes causes imbalance in chemical reaction and thus can affect the performance of battery.

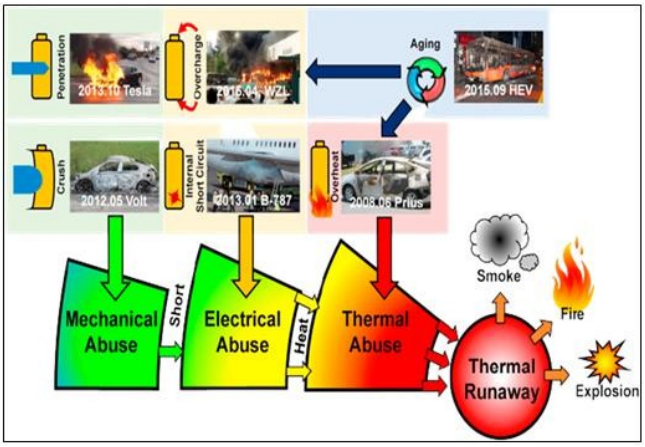

Fig.2. Thermal runaway in Li-ion batteries [11]

In order to tackle these heating issues of battery, there is a need for development of efficient Battery Thermal Management System (BTMS) which can keep the battery pack within safe operating limit. An implementation of proper BTMS, along the battery pack arrangement can help to mitigate the impact due to rising temperature of battery pack. The BTMS structure may differ depending upon the layout of battery pack and its size. There is different battery cooling techniques that are adopted by researchers and automotive manufactures over the globe.[12] The different battery cooling techniques are as follows Air cooling, Liquid cooling, Phase Change Material (PCM) cooling, Heat Pipe cooling and Immersion cooling. An air-cooled battery thermal management system (BTMS) is a technique used to regulate and control the temperature of batteries by utilizing air as the cooling medium. This method involves the circulation or forced flow of ambient air over the battery pack to dissipate heat and maintain optimal temperature conditions. A phase change material (PCM) battery cooling system is a thermal management technique that utilizes phase change materials to regulate and dissipate heat from batteries. [13] A large amount of heat can be absorbed or released using phase change material during phase transitions, providing efficient and effective cooling for battery systems. A heat pipe cooling system is a thermal management technique that utilizes heat pipes to transfer and dissipate heat from a heat source, such as a battery or electronic component. Heat pipes are highly efficient heat transfer devices that rely on the principles of phase change and thermal conductivity to transport heat over long distances with minimal temperature differences. A liquid-cooled battery thermal management system is a technology used to regulate and maintain optimal operating temperatures for batteries by using a liquid coolant. This system typically consists of a network of channels or pipes that circulate a coolant, such as water or a specialized fluid, throughout the battery pack. The coolant absorbs heat generated during battery operation and transfers it away from the cells, helping to regulate their temperature. [14] The different coolants used in Battery Thermal Management System (BTMS) for EVs and which play a crucial role in maintaining optimal operating temperatures for the vehicle battery are water-ethylene glycol mixtures, dielectric fluids, refrigerants and other ionic liquids. [15] The use of ethylene glycol which can be added to water to form a coolant having good thermal properties and are widely used in automotive applications. High thermal stability, non-flammable nature and good dielectric properties make the use of fluorinated fluids such as perfluoropolyether (PFPE) suitable for use as coolant. The use of refrigerants as coolants is also focused upon due to its impact in automotive air conditioning cycle and thus refrigerants with lesser potential to global warming are selected. The good thermal properties exhibited by fluids containing ionic salts making the solution non-volatile and suitable for use in as coolant in BTMS.

IV. ANALYTICAL APPROACH

The analytical approach starts with the calculation of heat generation in a single cell at different charge-discharge rates and later in the battery pack using Joule's heating and Bernardi equation. The constant surface temperature of the battery pack can be calculated at different C-rates using simple relation between the heat generated in battery and the battery performance parameters along with some electrical parameters. Once the heat generated in battery pack is known the battery cooling channels for flow, the coolant through the system is finalized. The thermo physical properties of silicon dioxide nanoparticles at 27 ° C along with base fluids are mentioned in detail. The heat balance equations are applied in equating the convective heat transfer to the heat absorbed by the fluid flowing through the cooling channel. The concept of log mean temperature difference is applied for calculating the outlet temperature of coolant under test. The best base fluid is selected based on the optimized temperature reduction value of battery pack after cooling.

A. MATHEMATICAL CALCULATIONS

The heat generation in battery pack can be calculated by the summation of heat generation in Joule's heating as well as in the Bernardi equation. [16] The heat generation in Joule's heating equation is due to flow of current and presence of resistive load across the system producing heat. The Bernardi equation is a widely used method for calculating the heat generation in lithium-ion batteries. It is based on the principle that the heat generation is equal to the sum of the reversible heat and the irreversible heat. The

 e-ISSN No. 2584-1025

reversible heat is the heat that is generated by the entropy change during the charging and discharging process, and the irreversible heat is the heat that is generated by the ohmic resistance of the battery. The relation for calculating the heat generation in single LFP cell can be expressed as follows in equation (1) and (2) [17]:

$$Q_{heat} = Joule's\ Heating + Bernardi\ Equation \quad (1)$$

$$Q_{heat} = I^2 \times R + I \times (U - V) \quad (2)$$

The open circuit voltage of LFP 32700 cells is 3.65 V, data taken from the specification sheet for the respective cells. The cell internal resistance is 0.010 Ω and the cell capacity is 3C discharge. The Table.1. Depicts the heat generation during charge-discharge at different C-rates for the battery pack using Joule's heating and Bernardi equation. The current study focuses on the use of Modified Indian Drive Cycle (MIDC) for 4 Wheeler to carry analytical calculations as well as validation using experimental approach. [18] The MIDC cycle consists of two parts, the part 1 includes four cycles from 0 to 195 seconds and part 2 consists of Extra Urban Driving Cycle (EUDC) for 400 seconds hereby having total testing cycle time of 1180 seconds.

Table.1.Heat generation during charge-discharge at different C-rates

C-rates	(V)	(O.C.V) (V)	(I) A	(R) Ω	($Q_{cell\ heat}$) (W)	Total cells (n)	($Q_{battery\ heat}$) (W)
Charge Rates							
0.3C	3.2	3.65	1.8	0.010	**0.8424**	105	**88.45**
0.6C	3.2	3.65	3.6	0.010	**1.7496**	105	**183.71**
1C	3.2	3.65	6	0.010	**3.06**	105	**321.3**
Discharge Rates							
1C	3.2	3.65	6	0.010	**3.06**	105	**321.3**
2C	3.2	3.65	12	0.010	**6.84**	105	**718.2**
3C	3.2	3.65	18	0.010	**11.34**	105	**1190.7**

The Fig.3. Shows the plot for Modified Indian Drive Cycle. The velocity vs. time plot of MIDC is converted into acceleration vs. time plot for establishing relation between acceleration of vehicle with the current drawn from the battery pack. The Fig.4. Depicts the acceleration vs. time plot for Part 1 of MIDC cycle. The above figure represents the relation of vehicle acceleration with time and value of current can be found out. The Fig.5. Depicts the acceleration vs. time plot for Part 2 of MIDC cycle. The relation between power required by the vehicle and current drawn from the battery pack can be expressed as follows in equation (3):

$$Power\ (P) = Voltage\ (V) \times Current\ (I) \quad (3)$$

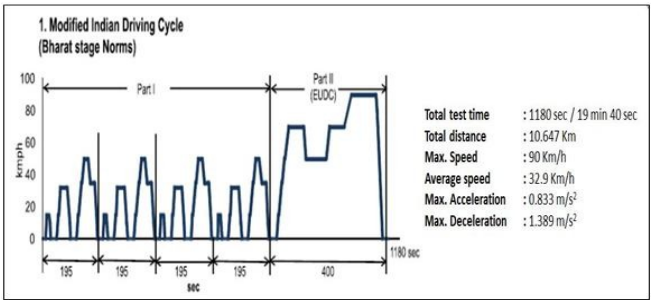

Fig.3. Shows the plot for Modified Indian Drive Cycle [18]

The current vs. time graph for the required MIDC cycle can be calculated by dividing the power required for each second during execution of drive cycle by the nominal voltage of the battery pack. The nominal voltage for the current battery pack is 48 V. The power required is calculated by multiplying the tractive force required per second to the velocity corresponding at that second. The battery pack selected for this study is 48 V 42 Ah which is chosen from a four wheeler manufactured for personal mobility application. The Table.2. Depicts the vehicle parameters for calculating the required tractive forces.

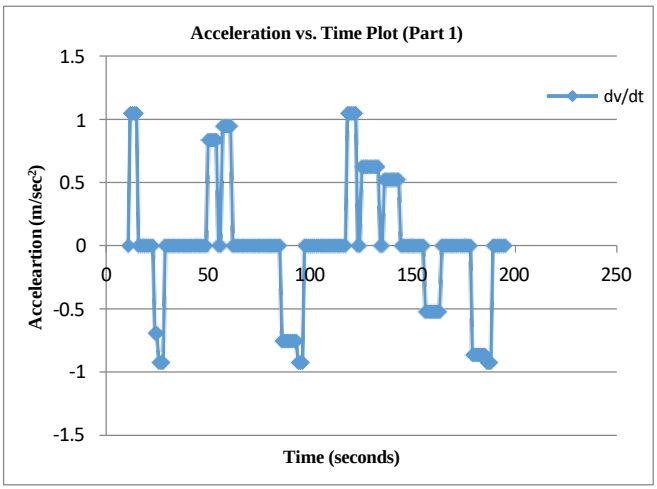

Fig.4. Depicts the acceleration vs. time plot for Part 1 of MIDC cycle

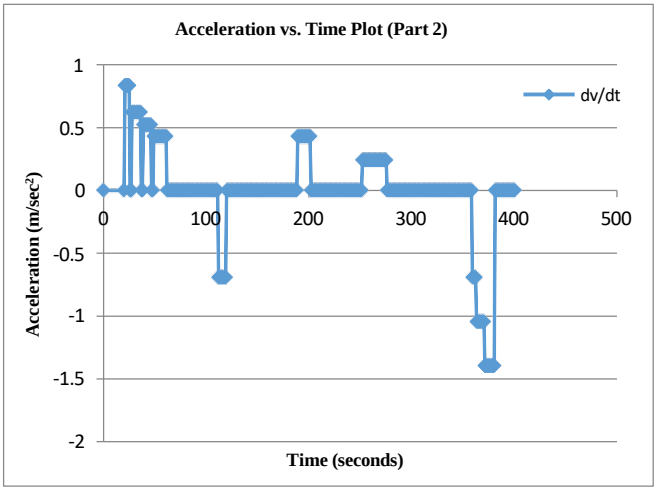

Fig.5. Depicts the acceleration vs. time plot for Part 2 of MIDC cycle

 e-ISSN No. 2584-1025

Table.2. Vehicle parameters for calculating the required tractive forces

Vehicle Parameters	Unit	Value
Mass (m)	kg	**575 + 68*2 = 711**
Acceleration due to gravity (g)	m/sec^2	**9.81**
Coefficient of Drag (Cd)	-	**0.4**
Rolling Resistance (μ_{rr})	-	**0.025**
Air Density (ρ)	kg/m^3	**1.25**
Area (W X H)	m^2	**1.157*1.600 = 1.85**

The tractive force is the summation of rolling resistance, aerodynamic drag and acceleration forces. [19] The hill climbing force in this case is neglected. The equation (4) and (5) express the total tractive force in terms of summation of others forces along with the power required is as follows:

$$F_t = F_r + F_d + F_a \quad (4)$$

$$Power\ (P) = Tractive\ Force\ (F_t) \times Velocity\ (v) \quad (5)$$

By applying these equations to the velocity vs. time data from the drive cycle along with vehicle parameters, the values of tractive forces, power required and the current value corresponding to the power per second can calculated in excel software. The current vs. time plot can be obtained from the table described above. Once the graph of current vs. time plot is obtained for 0 to 195 seconds MIDC, the regions of maximum current can be identified. The temperature at these current values can be calculated using a simple principle that the heat generated by the battery cell is proportional to the current and voltage, and inversely proportional to the capacity and thermal constant. Thus, the temperature of battery cell (Tb) can be represented as follows in equation (6) and Table.3. Depicts Temperature value for different C-rates,

$$T_{cell}\ (^oC) = T_{ambient}\ (^oC) + \frac{(I \times V \times R)}{C \times T_{constant}} \quad (6)$$

Table.3. Depicts Temperature values for different C-rates

1 C	2 C	3 C
T cell = 34° C	T cell = 41 ° C	T cell = 47 ° C

The Fig.6. Represents the plot for current vs. time for MIDC (Part-1). The Fig.7. Represents the plot for current vs. time for MIDC (Part-2). The maximum working temperatures from MIDC Part-1 and MIDC-Part-2 can be found out from current vs. time plot. The current range for 1C discharge can be seen from plot is to be from 39 A to 44 A. Also the current range for 2C discharge can be seen from plot is to be from 76 A to 87 A. The current range for 3C discharge can be seen from plot is to be from 126 A to 141 A. The maximum current can be reached up to 200 A, but the current drawn is for less time interval. The different base fluids used for preparation of nanofluids are water, ethylene glycol (EG) or mixture of water-ethylene glycol. The different thermo physical properties of these base fluids are mentioned in [20] [21] Table.4. Currently mixture of water-ethylene glycol is used by manufactures for battery cooling applications in EVs due to advantages it offers. However, the performance of cooling is not satisfactory causing difficulty in maintaining the battery pack temperature within operating temperature limits. [22] However the thermo physical properties of these nanofluids can be found out using co-relations as follows in equation (7) (8) (9) and (10). [23] [24] The thermo physical properties of silicon dioxide nanoparticles used in battery cooling applications are mentioned in Table.5.

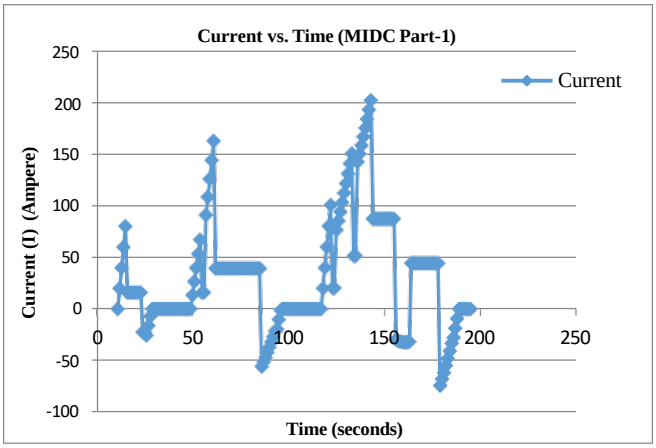

Fig.6. Represents the plot for current vs. time for MIDC (Part-1)

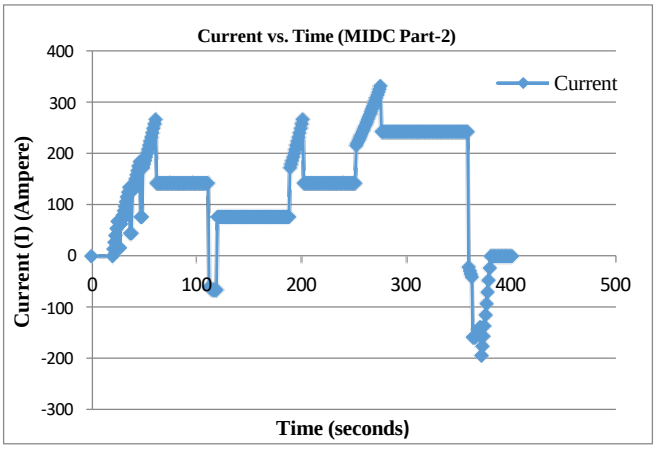

Fig.7. Represents the plot for current vs. time for MIDC (Part-2)

Table.4. Thermo Physical properties of Base fluids (300 K) [21, 22]

Sr. No.	Base Fluids	Thermal Conductivity (W/mK)	Viscosity (mPasec)	Density (kg/m^3)	Specific Heat Capacity (J/kg K)	Freezing Point Temperature (^{o}C)	Boling Point Temperature (^{o}C)
1	Water	0.609	0.850	996	4180	0	100
2	EG	0.257	15.5	1130	2408	-12.8	197.3
3	50:50 Water -EG	0.433	2.8	1077	3495	-36.8	107
4	60:40 Water -EG	0.468	2.2	1060	3665	-23.5	106
5	70:30 Water -EG	0.503	1.7	1048	3822	-13.7	104
6	80:20 W-EG	0.538	1.5	1040	3963	-7.9	102

Thermal Conductivity:

$$K_{nf} = \frac{2K_{bf}+K_{np}+2\emptyset(K_{np}-K_{bf})}{2K_{bf}+K_{np}-\emptyset(K_{np}-K_{bf})}(K_{bf}) \quad (7)$$

Density:

$$\rho_{nf} = \emptyset(\rho_{np}) + (1-\emptyset)(\rho_{bf}) \quad (8)$$

Specific Heat Capacity:

$$Cp_{nf} = \emptyset(Cp_{np}) + (1-\emptyset)(Cp_{bf}) \quad (9)$$

Viscosity:

$$\mu_{nf} = (1+2.5\emptyset)\mu_{bf} \quad (10)$$

Table.5. Thermo physical properties of aluminium oxide Nanoparticles (300 K) [21-25]

Sr.No.	Nanoparticles	Thermal Conductivity (W/mK)	Density of Fluid (kg/m^3)	Specific Heat Capacity (J/kgK)
1	Silicon Dioxide	1.2	2200	745

The heat transfer calculations carried out for different nanofluids discussed in this paper and are tabulated for estimating better cooling performance. The formulas for calculating outlet temperature of fluid flow through the cooling channel are discussed considering the flow regime of fluid to be laminar or turbulent.[25] The formula for calculating mass flow rate, Reynolds number, Prandtl number, Nusselt number and eventually the heat transfer coefficient are as follows in equations (11) (12) (13) (14) (15) (16) and heat balance equations in (17) (18) respectively, :

Mass Flow Rate (m):

$$m = \frac{\pi\times\rho\times D^2\times v}{4} \quad (11)$$

Reynolds Number (Re)

$$Re = \frac{4\times m}{\pi\times D\times\mu} \quad (12)$$

Prandtl Number (Pr)

$$Pr = \frac{\mu\times C_p}{k} \quad (13)$$

The value of Nusselt Number is calculated by relating Reynolds's number and Prandtl Number values as below,

For Laminar Flow (Sieder and Tate 1936):

$$Nu = 1.86 \times [Re\times Pr\times(\frac{D}{L})]^{\frac{1}{3}}\times(\frac{\mu}{\mu_w})^{0.14} \quad (14)$$

When, $13 \le Re \le 2300$, $0.48 \le Pr \le 16700$, $0.0044 \le \frac{\mu}{\mu_w} \le 9.75$

For Turbulent Flow (Whitaker correlation 1972):

$$Nu = 0.015 \times Re^{0.83}\times Pr^{0.42}\times(\frac{\mu}{\mu_w})^{0.14} \quad (15)$$

When, $2300 \le Re \le 1 * 10^5$, $0.48 \le Pr \le 592$, $0.44 \le \frac{\mu}{\mu_w} \le 2.5$

Heat Transfer Coefficient (h):

$$h = \frac{Nu\times k}{D} \quad (16)$$

Heat Balance Equation:

Convective Heat Transfer = Heat absorbed by Fluid

$$h \times A_s \times \Delta T_{lm} = m \times C_p \times (\Delta T_i - \Delta T_o) \quad (17)$$

Where,

$$\Delta T_i = T_{surface} - T_{inlet}\ ,\ \Delta T_o = T_{surface} - T_{outlet}$$

$$\Delta T_{lm} = \frac{(\Delta T_o - \Delta T_i)}{\ln(\frac{\Delta T_o}{\Delta T_i})}$$

Final Equation for calculating the outlet temperature of fluid is as follows:

$$T_{0utlet} = T_{surface} - (T_{surface} - T_{inlet}) \times e^{-(\frac{h \times A_s}{m \times Cp})} \quad (18)$$

V. RESULTS AND DISCUSSIONS

The thermo physical properties of silicon dioxide nanofluids for 5 % particle concentration are found using analytical relations. The Table.6. Depicts thermo physical properties of Silicon dioxide (SiO_2) nanoparticles co-related with different base fluids.

Table.6. Depicts Silicon dioxide (SiO_2) nanoparticles co-related with different base fluids

Sr.No.	Nanofluids Φ = 5 %	Thermal Conductivity (W/mK)	Density (kg/m3)	Viscosity (mPasec)	Specific Heat Capacity (J/kgK)
1	Silicon Dioxide + Water	0.63	1056	0.96	4008
2	Silicon Dioxide + Ethylene Glycol	0.28	1183	17.40	2325
3	Silicon Dioxide + 50:50 Water & Ethylene glycol	0.46	1133	3.15	3357
4	Silicon Dioxide + 60:40 Water & Ethylene glycol	0.49	1117	2.48	3519
5	Silicon Dioxide + 70:30 Water & Ethylene glycol	0.53	1105	1.91	3668
6	Silicon Dioxide + 80:20 Water & Ethylene glycol	0.56	1098	1.69	3802

Based on the thermo physical properties of silicon dioxide nanofluids at 5 % particle concentrations, the cooling performance of the nanofluid may vary. The Table.7. Represents the Battery reduction temperature using silicon dioxide nanofluid at 5 % particle concentration. Based on the battery temperature reduction values obtained using heat transfer equations for different base fluids, the most effective cooling performance is obtained using water as base fluid and least cooling performance is obtained for ethylene glycol base fluid. However, the use of water is restricted as base fluid in the operating regions that can vary from colder climatic conditions to hotter climatic conditions resulting in solidification or evaporation of water leading to inefficient performance of coolant. The ethylene glycol is however preferred due to low cost but the performance of cooling is not effective as in comparison with mixture of water-ethylene glycol. Thus, through optimal analysis the best base fluid chosen is 70:30 water-ethylene glycol mixture, having temperature reduction of 39.94 ºC with freezing and boiling temperatures of -13.7 ºC and 104 ºC respectively suited for battery cooling applications.

Table.7. Represents the Battery temperature reduction for silicon dioxide nanofluid at 5% concentration

Sr.No	Nanofluids (Φ = 5 %)	Battery Temperature Reduction (ºC)
1	Silicon Dioxide + Water	39.54
2	Silicon Dioxide + Ethylene Glycol	44.81
3	Silicon Dioxide + 50:50 Water & Ethylene glycol	41.21
4	Silicon Dioxide + 60:40 Water & Ethylene glycol	40.64
5	Silicon Dioxide + 70:30 Water & EG	39.94
6	Silicon Dioxide + 80:20 Water & Ethylene glycol	39.59

VI. CONCLUSION AND FUTURE SCOPE

The current paper addressed the problem related to thermal runaway in LFP battery pack. As the LFP battery pack works well within certain range of operating temperatures and thus temperatures above or below this range can affect the performance of battery pack. Currently used coolants in battery cooling applications are water, ethylene glycol and mixture of water-ethylene glycol. However, the performance of cooling is not satisfactory and thus there is a need to focus on different coolants for battery cooling applications. The best suited base fluid from the analytical calculations was found out to be 70:30 water-ethylene glycol mixtures having higher temperature reduction value when used as coolant. The future scope of the work also lies in validating the analytical results obtained for silicon dioxide nanofluids at different velocities and comparing it using the results obtained through experimental analysis.

ACKNOWLEDGMENT

A heartfelt thank you by authors to School of Engineering and Sciences at MIT-ADT University for complete guidance throughout the course of study.

REFERENCES

[1] F. Un-Noor, S. Padmanaban, L. Mihet-Popa, M. N. Mollah, and E. Hossain, "A comprehensive study of key electric vehicle (EV) components, technologies, challenges, impacts, and future direction of development," *Energies*, vol. 10, no. 8, 2017, doi: 10.3390/en10081217.

[2] A. Faraz, A. Ambikapathy, S. Thangavel, K. Logavani, and G. Arun Prasad, "Battery Electric Vehicles (BEVs)," *Green Energy Technol.*, no. January 2021, pp. 137–160, 2021, doi: 10.1007/978-981-15-9251-5_8.

[3] F. Monti, A. Barbieri, and N. Armaroli, "Battery Electric Vehicles: Perspectives and Challenges," *Substantia*, vol. 3, no. 2, pp. 75–89, 2019, doi: 10.13128/Substantia-576.

[4] J. Du and D. Ouyang, "Progress of Chinese electric vehicles industrialization in 2015: A review," *Appl. Energy*, vol. 188, pp. 529–546, 2017, doi: 10.1016/j.apenergy.2016.11.129.

[5] J. Speirs, M. Contestabile, Y. Houari, and R. Gross, "The future of lithium availability for electric vehicle batteries," *Renew. Sustain. Energy Rev.*, vol. 35, pp. 183–193, 2014, doi: 10.1016/j.rser.2014.04.018.

[6] J. Jaguemont, L. Boulon, and Y. Dubé, "A comprehensive review of lithium-ion batteries used in hybrid and electric vehicles at cold temperatures," *Appl. Energy*, vol. 164, pp. 99–114, 2016, doi: 10.1016/j.apenergy.2015.11.034.

[7] O. Toprakci, H. A. K. Toprakci, L. Ji, and X. Zhang, "28_2010008," vol. 28, no. 28, pp. 50–73, 2010.

[8] M. Wang *et al.*, "Recycling of lithium iron phosphate batteries: Status, technologies, challenges, and prospects," *Renew. Sustain. Energy Rev.*, vol. 163, no. April, 2022, doi: 10.1016/j.rser.2022.112515.

[9] X. Feng, D. Ren, X. He, and M. Ouyang, "Mitigating Thermal Runaway of Lithium-Ion Batteries," *Joule*, vol. 4, no. 4, pp. 743–770, 2020, doi: 10.1016/j.joule.2020.02.010.

[10] B. Xu, J. Lee, D. Kwon, L. Kong, and M. Pecht, "Mitigation strategies for Li-ion battery thermal runaway: A review," *Renew. Sustain. Energy Rev.*, vol. 150, no. October 2020, p. 111437, 2021, doi: 10.1016/j.rser.2021.111437.

[11] X. Feng, M. Ouyang, X. Liu, L. Lu, Y. Xia, and X. He, "Thermal runaway mechanism of lithium ion battery for electric vehicles: A review," *Energy Storage Mater.*, vol. 10, no. December 2016, pp. 246–267, 2018, doi: 10.1016/j.ensm.2017.05.013.

[12] T. I. C. Buidin and F. Mariasiu, "Battery thermal management systems: Current status and design approach of cooling technologies," *Energies*, vol. 14, no. 16, 2021, doi: 10.3390/en14164879.

[13] M. M. Hamed, A. El-Tayeb, I. Moukhtar, A. Z. El Dein, and E. H. Abdelhameed, "A review on recent key technologies of lithium-ion battery thermal management: External cooling systems," *Results Eng.*, vol. 16, no. October, p. 100703, 2022, doi: 10.1016/j.rineng.2022.100703.

[14] R. Youssef, T. Kalogiannis, H. Behi, A. Pirooz, J. Van Mierlo, and M. Berecibar, "A comprehensive review of novel cooling techniques and heat transfer coolant mediums investigated for battery thermal management systems in electric vehicles," *Energy Reports*, vol. 10, pp. 1041–1068, 2023, doi: 10.1016/j.egyr.2023.07.041.

[15] Y. Deng *et al.*, "Effects of different coolants and cooling strategies on the cooling performance of the power lithium ion battery system: A review," *Appl. Therm. Eng.*, vol. 142, no. June, pp. 10–29, 2018, doi: 10.1016/j.applthermaleng.2018.06.043.

[16] J. Zhang, X. G. Yang, F. Sun, Z. Wang, and C. Y. Wang, "An online heat generation estimation method for lithium-ion batteries using dual-temperature measurements," *Appl. Energy*, vol. 272, no. December 2019, p. 115262, 2020, doi: 10.1016/j.apenergy.2020.115262.

[17] N. H. F. Ismail, S. F. Toha, N. A. M. Azubir, N. H. Md Ishak, M. K. Hassan, and B. S. Ksm Ibrahim, "Simplified heat generation model for lithium ion battery used in electric vehicle," *IOP Conf. Ser. Mater. Sci. Eng.*, vol. 53, no. 1, 2013, doi: 10.1088/1757-899X/53/1/012014.

[18] https://www.araiindia.com/CMVR_TAP_Documents/Part-14/Part-14_Chapter03.pdf

[19] S. Wankhede, P. Thorat, S. Shisode, S. Sonawane, and R. Wankhade, "Energy consumption estimation for electric two-wheeler using different drive cycles for achieving optimum efficiency," *Energy Storage*, vol. 4, no. 6, 2022, doi: 10.1002/est2.361.

[20] P. Thorat, "Experimental investigation of change in performance parameters on cooling of lithium-ion battery pack using nanofluids," *Energy Storage*, vol. 5, no. 6, pp. 1–14, 2023, doi: 10.1002/est2.451.

[21] H. A. Hasan *et al.*, "Numerical investigation on cooling cylindrical lithium-ion-battery by using different types of nanofluids in an innovative cooling system," *Case Stud. Therm. Eng.*, vol. 49, no. May, p. 103097, 2023, doi: 10.1016/j.csite.2023.103097.

[22] X. Xu, T. Xiao, S. Chen, and S. Lin, "Exploring the heat transfer performance of nanofluid as a coolant for power battery pack," *Heat Transf. - Asian Res.*, vol. 48, no. 7, pp. 2974–2988, 2019, doi: 10.1002/htj.21526.

[23] P. Kanti, K. V. Sharma, M. Revanasiddappa, C. G. Ramachandra, and S. Akilu, "Thermophysical properties of fly ash–Cu hybrid nanofluid for heat transfer applications," *Heat Transf.*, vol. 49, no. 8, pp. 4491–4510, 2020, doi: 10.1002/htj.21837.

[24] S. Akilu, A. T. Baheta, K. V. Sharma, and M. A. Said, "Experimental determination of nanofluid specific heat with SiO2 nanoparticles in different base fluids," *AIP Conf. Proc.*, vol. 1877, 2017, doi: 10.1063/1.4999896.

[25] https://www.studocu.com/en-za/document/university-of-the-witwatersrand-johannesburg/thermodynamics/4-evaluation-of-transfer-coefficients-enginee-2007-modeling-in-transport/3661002